Cascaded Multilevel Inverter for PV-Active Power Filter Combination into the Grid-Tied Solar System

Mariem Tayari‡, Abdessettar Guermazi, Moez Ghariani

Electric Department, national school of engineering in Sfax, laboratory of advanced electronic systems and sustainable energy, University of Sfax, 3038

(tmariem48@yahoo.com, guermazi.abs@gmail.com, moez.ghariani@gmail.com)

‡
Mariem Tayari, Postal address, Tel: +216 29 902 301, tmariem48@yahoo.com

Received: 17.09.2020 Accepted:12.10.2020

Abstract- The presence of non-linear loads, such as electronic power converter, into the grid generally affects the electric power quality. This latter presents a fundamental factor in the performance of the grid consumers. Besides, nowadays, the photovoltaic (PV) energy integration spreads for residential and commercial applications. These PV systems impose the use of power inverters to liaise with the electric grid. In this context, this paper aims to benefit from a modelling PV inverter to fix the power disorder and then to guarantee better equipment performance. The proposed model configuration mainly involves a seventeen-level cascaded inverter controlled by the active and reactive instantaneous power theory. The regulation system consists of PI regulators for the dc-link voltage as well as the inverter output currents. This PV inverter provides successful harmonics mitigation while achieving its fundamental function. Also, it ensures reduction of overall source current THD values, efficient DC-link regulation, and quick response over the system variations. MATLAB/Simulink simulation results show the electrical behaviour of the whole model for different cases and operation modes.

Keywords the grid-tied solar system, multilevel inverter, instantaneous power theory, harmonic mitigation, DC voltage balancing, reactive power reduction.

1. Introduction

Nowadays, centralized power generation systems are facing a scarcity of non-renewable resources. Furthermore, the excess demand for electricity stimulates to find new production systems which need to provide more power, greater efficiency, and less pollution. Thus, electricity companies are moving toward integrating renewable energy conversion systems (wind energy conversion systems, PV conversion systems). As well, PV systems occupy a fundamental place in electricity production. That is thanks to several factors; reducing costs, increasing yield, searching for an alternative clean energy source, and encouraging environmental awareness. Thus, that leads to the enormous growth of the use of the PV conversion systems. One of its most well-known configurations is the grid-tied solar system which accounts for over 99 % of the installed PV system capacity[1]. It is because of no need for batteries as the case of the stand-alone structure. The grid-tied solar system principle is to direct delivering of the PV power to the electric grid. Thus, abandoning the use of such batteries ensures the cost optimization, the effectiveness improvement, and the reduction of the maintenance and re-investment costs.

Figure 1 depicts the structure of the grid-tied solar system[2]. A PV inverter is necessary to deliver the solar panels energy to the electric network. The connection of this power stage with the DC energy source can be either with or without a DC-DC converter. On the other side of the PV inverter, a passive filter is essential for the connection to the electric grid. But, the intermittent nature of PV systems disturbs the

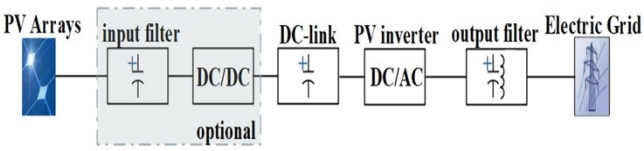

Fig. 1. The grid-tied solar system structure

electricity quality. This issue may arise with the excessive use of non-linear loads into the grid. It is the cause of harmonic currents production which lead then to generating harmonics voltages via grid impedances. They affect not only the grid but also the different consumers attached to it. These perturbations trigger annoying effects such as the excessive neutral currents, inaccuracies in the measuring system, overheating, protective relay, and circuit breakers operation failure, capacitor blowing, motor vibration, etc.[3] So, the purpose is to keep high-quality power by mitigating these existed perturbations. One of the solutions for this such power disorder is the parallel active power filter. The latter's main characteristic is the proficiency. But the high cost presents its principal drawback.

Thus, as a solution to minimize the costs, researchers suggest applying an adjustment in the PV inverter structure to obtain a multi-functional system which provides the feasibility to mitigate electric perturbations besides delivering PV system energy[4], [5]. For the power system, the selected topology is a multilevel inverter that proves its efficiency in the medium to high power applications. These advanced power system topologies are more suitable for the active power filters as well as the PV inverters than the traditional inverters[6], [7]. Among the several multilevel structures, the cascaded H-bridge inverter is the best adapted for PV systems since each photovoltaic array or panel can act as a separate direct current source for each H-bridge cell.[8]–[10] Also, to achieve this inverter multi-function, its control flexibility plays the principal role.[11]

The first objective, in this paper, is the performance checking of the proposed structure. The verification applied by its comparison to another PV inverter with the same topology and in the same operating conditions. It helps to distinguish the strengths and vulnerabilities of the new model. After the efficiency validation, another point needs to be made about one of the disadvantages of the cascaded multilevel inverter use for this application. It is the dependence on the number of PV arrays, contrary to the traditional topology of PV inverter. Thus, the second objective, of this paper, is modelling a modular cascaded inverter that can operate with the different number of cells while depending for the existing PV arrays.

The paper organization is as follows. The second section presents a brief description of the whole studied-system design. It is about the description of the power stage model and its control system. The third section is dedicated to the evaluation of the proposed PV inverter. It includes simulated test cases through the MATLAB/Simulink platform. The summarized results are outlined in the conclusion section.

2. The System Design

Figure 2 shows the entire system illustration, stating the PV inverter configuration. It is a modular cascaded multilevel inverter. It consists in the connection of each H-Bridge cell with a PV panel through a DC-DC converter. A passive filter is an interface between the other side of the PV inverter and the electric network. Beyond the solar conversion system, there are various loads connected to the grid. The following sections present a detailed description of each part of this system.

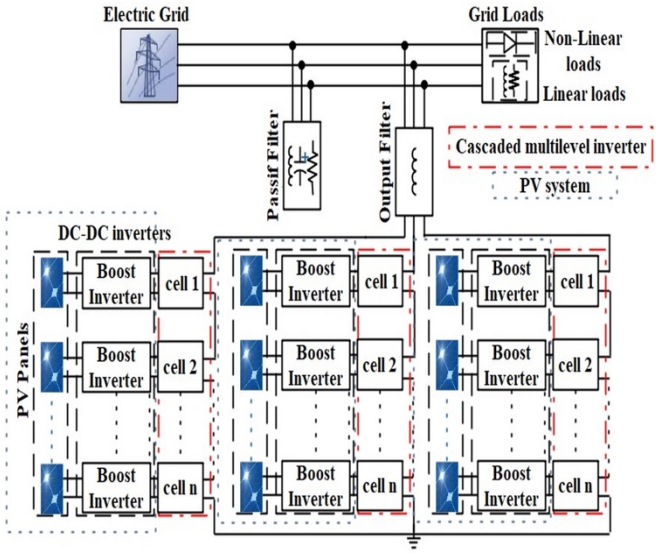

Fig. 2. The studied system architecture

2.1. The PV system

The PV system consists of PV panels connected to the DC-DC converter that fix the amount of energy delivered by the PV panels. This converter controller compels the PV panel to generate the maximum available power. Thus, the use of a Maximum Power Point Tracking (MPPT) algorithm as a control technique is required. The most known MPPT algorithms are the incremental conductance (INC) and the perturbation-observation (P&O) methods. The second MPPT technique is widely used in practice due to many factors. There is the easy implementation, the compromise between simplicity and efficiency.[12]–[15] Figure 3 illustrates the principle of the proposed method.

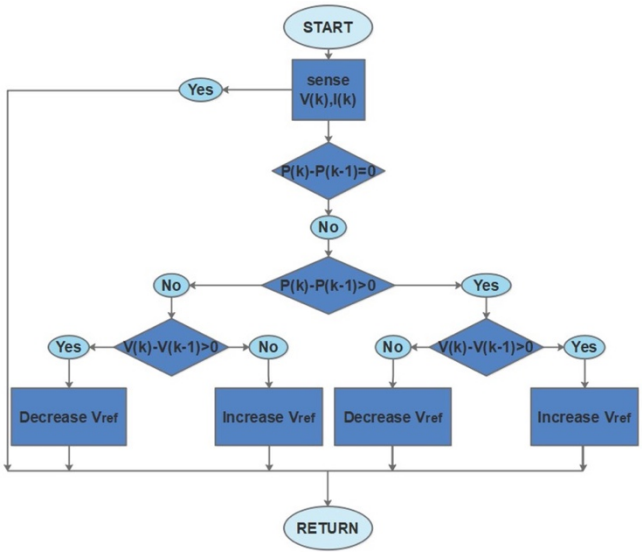

Fig. 3. The P&O method flowchart

It involves a variation of the operating voltage of the DC link between the power converter to the PV panel. The signs of the last voltage variation and power increment are the inputs to extract the new voltage value[16]. The MPPT output voltage is the reference voltage to control the boost converter.

2.2. The PV Inverter

The electricity production has seen an enormous growth of the PV systems use. That has sparked a continuous progression of its different components to achieve extreme efficiency, compactness, and reliability. Thus, the PV system market lays down exaggerated requirements; warranty periods for a long time, high efficiency (above 98%), high power quality, minimized leakage current, and transformerless operation.[1], [17] That leads to explore multilevel inverters, to meet the market demand. It is one of the alternative solutions used for high-power applications. This choice is justified by several advantages such as higher voltage operating capability, lower common-mode voltages, near sinusoidal absorbed or injected current, smaller input and output filters if necessary, increased efficiency, possible fault-tolerant operation (in some cases).[18] Also, these power electronic devices enable the direct connection between the megawatt grid and the solar conversion system. Among the most known multilevel inverter topologies, there is the cascaded inverter. It attains the higher power levels and output voltages than other multilevel structures. Furthermore, its modular topology allows for higher reliability. The cascaded multilevel inverter consists of a series connection of H-bridge inverters that leads to reach a high modularity degree. These single-phase cells have the same structure and the same control circuit. Thus, in case of a defect in one of those modules, its replacement would be easy and fast. Moreover, the work-in-process system is not affected while bypassing the defective module.

The cascaded n-level inverter consists of (n-1)/2 cells per phase. The basic structure of each cell is an H-bridge inverter with a capacitor acting as a DC source. The output voltage waveform of this latter is a quasi-square wave with (+ Vdc, 0, -Vdc) output levels. For each phase, the ac terminal voltages of different cells need to be in series connection. Thus, the inverter final output voltage is the sum of the each-phase cells output voltages.

Also, the used PV inverter has a transformerless structure. This choice is on account of the drawbacks encountered in the use of transformers. There is the high cost, the increase of the power losses, and its high susceptibility to failure.

The proposed system is a seventeen-level cascaded multilevel inverter shown in figure 4.

$e_{r1,2,3}$, $i_{r1,2,3}$	Three-phase grid voltages and currents
(L_r,R_r), (L_f,R_f)	Grid, output filter impedances
$V_{r1,2,3}$	Three-phase voltages at the PCC point
$Vc(i,j)$	Dc-link voltage corresponding to cell j in phase i
T_1, T_2 (i,j)	Control signals of cell i in the phase j
$V_{h1,2,3}$, $i_{h1,2,3}$	Three-phase PV inverter voltages and currents

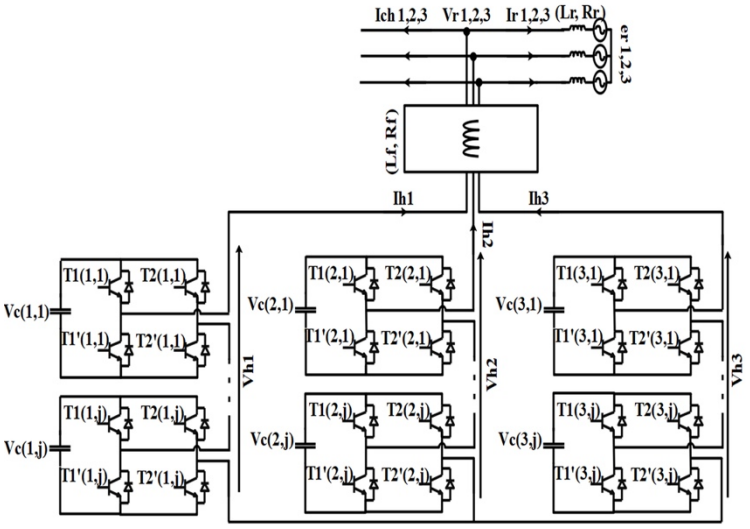

Fig. 4. The model of the cascaded multilevel inverter with (2j+1) levels connected to the grid

The mathematical representation of a five-level cascaded inverter after the Clarke transformation is as below.

$$\frac{d}{dt}[I_h]=\frac{d}{dt}\begin{pmatrix}I_{h\alpha}\\I_{h\beta}\end{pmatrix}=\frac{1}{L_f}\left(\begin{pmatrix}V_{h\alpha}\\V_{h\beta}\end{pmatrix}-\begin{pmatrix}V_{r\alpha}\\V_{r\beta}\end{pmatrix}-R_f\begin{pmatrix}I_{h\alpha}\\I_{h\beta}\end{pmatrix}\right) \quad (1)$$

$$\frac{d}{dt}[I_r]=\frac{d}{dt}\begin{pmatrix}I_{r\alpha}\\I_{r\beta}\end{pmatrix}=\frac{1}{L_r}\left(-R_f\begin{pmatrix}I_{h\alpha}\\I_{h\beta}\end{pmatrix}-\begin{pmatrix}V_{r\alpha}\\V_{r\beta}\end{pmatrix}+\begin{pmatrix}e_{r\alpha}\\e_{r\beta}\end{pmatrix}\right) \quad (2)$$

$$\frac{d}{dt}[V_C]=\frac{d}{dt}\begin{pmatrix}V_C(1,1) & V_C(1,2) & V_C(2,1) & V_C(2,2) & V_C(3,1) & V_C(3,2)\end{pmatrix}^T=B_1[U] \quad (3)$$

$$B_1=\frac{-1}{C}\begin{pmatrix}I_{h\alpha} & 0 & 0 & 0 & 0 & 0\\ 0 & I_{h\alpha} & 0 & 0 & 0 & 0\\ 0 & 0 & \frac{-I_{h\alpha}+\sqrt{3}I_{h\beta}}{2} & 0 & 0 & 0\\ 0 & 0 & 0 & \frac{-I_{h\alpha}+\sqrt{3}I_{h\beta}}{2} & 0 & 0\\ 0 & 0 & 0 & 0 & \frac{-I_{h\alpha}-\sqrt{3}I_{h\beta}}{2} & 0\\ 0 & 0 & 0 & 0 & 0 & \frac{-I_{h\alpha}-\sqrt{3}I_{h\beta}}{2}\end{pmatrix}$$

Using (1), (2), and (3), the space-state representation is:

$$\frac{d}{dt}X=AX+B(X)[U]+H[W] \quad (4)$$

$$X=\begin{bmatrix}[V_c]\\[I_h]\\[I_r]\end{bmatrix} \quad (5)$$

$$A=\begin{pmatrix} 0 & . & . & 0 \\ . & . & . & . \\ . & & 0 & 0 \\ 0 & . & 0 & A_1 \end{pmatrix} \quad (6)$$

$$A_1=\begin{pmatrix} -R_f/L_f & 0 & 0 & 0 \\ 0 & -R_f/L_f & 0 & 0 \\ 0 & 0 & -R_r/L_r & 0 \\ 0 & 0 & 0 & -R_r/L_r \end{pmatrix}$$

$$B(X)=\begin{pmatrix} B_1(X) \\ B_2(X) \\ 0 \\ 0 \end{pmatrix} \quad (7)$$

$$B_1(X)=B_1$$

$$B_2(X)=\frac{1}{L_f}\begin{pmatrix} \frac{2V_c(1,1)}{3} & \frac{2V_c(1,2)}{3} & \frac{-V_c(2,1)}{3} & \frac{-V_c(2,2)}{3} & \frac{-V_c(3,1)}{3} & \frac{-V_c(3,2)}{3} \\ 0 & 0 & \frac{V_c(2,1)}{\sqrt{3}} & \frac{V_c(2,2)}{\sqrt{3}} & \frac{-V_c(3,1)}{\sqrt{3}} & \frac{-V_c(3,2)}{\sqrt{3}} \end{pmatrix}$$

$$H=\begin{pmatrix} 0 & . & . & 0 \\ . & . & & . \\ . & & . & . \\ 0 & . & . & 0 \\ -1/L_f & 0 & 0 & 0 \\ 0 & -1/L_f & 0 & 0 \\ -1/L_r & 0 & 1/L_r & 0 \\ 0 & -1/L_r & 0 & 1/L_r \end{pmatrix}, \; W=\begin{bmatrix} [V_r] \\ [e_r] \end{bmatrix} \quad (8)$$

2.3. The Control System

Figure 5 summarizes the PV inverter control system. It consists of 3 principle circuits; harmonic compensation controller, DC bus regulator, and current regulator[19]. In the following parts, we presented a brief description of these blocs.

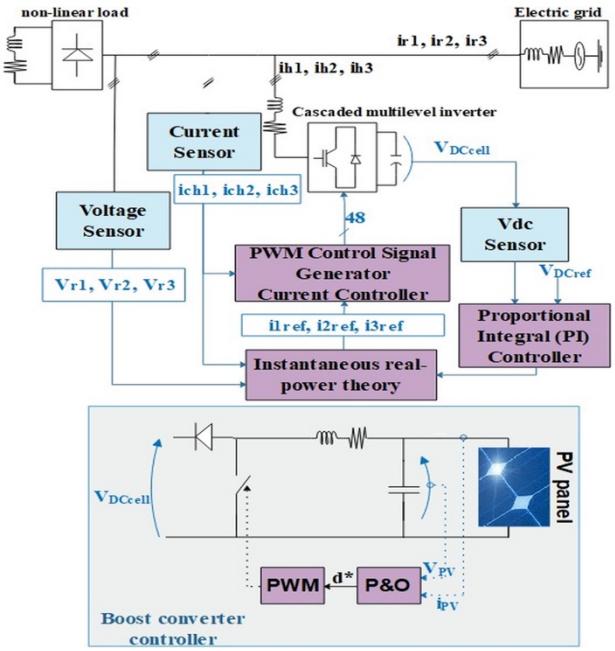

Fig. 5. Illustration of the entire control system

➢ *The harmonic compensation controller*

The inverter integrated by an APF-PV function should ensure the harmonics mitigation and simultaneously inject the PV system power [20]. Thus, the control system uses the instantaneous power technique. For this theory, all the parameters are tracked instantaneously via electric sensors. There are the voltages at the PCC point, the load, the grid and the inverter currents, and the dc-link voltages. The principle of this technique depends on the power balance at the PCC point.

P_{ch}, Q_{ch} Active and Reactive powers of the load
P_r, Q_r Active and Reactive powers of the grid
P_h, Q_h Active and Reactive powers of the PV inverter
p_{loss} Power corresponding to the PV inverter losses

$$\begin{cases} P_{ch}=P_r+P_h \\ Q_{ch}=Q_r+Q_h \end{cases} \quad (9)$$

The following expressions show the conventional instantaneous powers formulas extracted by Concordia transformation.

$$i_{\alpha\beta 0}(V_{\alpha\beta 0})=\sqrt{\frac{2}{3}}\begin{pmatrix} 1 & -1/2 & -1/2 \\ 0 & \sqrt{3}/2 & -\sqrt{3}/2 \\ 1/\sqrt{2} & 1/\sqrt{2} & 1/\sqrt{2} \end{pmatrix} i_{ch123}(V_{r123})$$

$$\begin{pmatrix} P_{ch} \\ Q_{ch} \end{pmatrix}=\begin{pmatrix} V_\alpha & V_\beta \\ -V_\beta & V_\alpha \end{pmatrix}\begin{pmatrix} i_\alpha \\ i_\beta \end{pmatrix}=\begin{pmatrix} \bar{p}_{ch}+\tilde{p}_{ch} \\ \bar{q}_{ch}+\tilde{q}_{ch} \end{pmatrix} \quad (10)$$

These latter include two components; average DC $^{-}$ and oscillating AC $^{\sim}$. Thus, a low pass filter (LPF) is necessary to decouple them. The used structure is a fifth-order Butterworth LPF.

For successful mitigation, the inverter should deliver the oscillating component of the real power as well as the imaginary power. In this case, the electric grid supplies either the total average power or only one fraction of it. That all depends on the PV inverter mode; either APF mode or APF-PV mode. Thus, the PV system generates the rest of the average power required by the load. An extra amount of active power p_{loss} is taken into consideration. It is the additional flow energy necessary to keep the DC-link voltages around a fixed value V_{dcref}. So, the reference injected powers can be expressed by:[21]

$$\begin{cases} P_{href}=\tilde{p}_{ch}-\bar{P}_r-p_{loss} \\ Q_{href}=Q_{ch}-\bar{Q}_r \end{cases} \text{ APF-PV mode}$$

$$\text{Or} \quad \begin{cases} P_{href}=\tilde{p}_{ch}-p_{loss} \\ Q_{href}=Q_{ch} \end{cases} \text{ APF mode} \quad (11)$$

After finding out the reference powers values, the corresponding currents are calculated by using the reverse Concordia transformation.

$$\begin{pmatrix} i_{h\alpha} \\ i_{h\beta} \end{pmatrix} = \frac{1}{V_\alpha^2 + V_\beta^2} \begin{pmatrix} V_\alpha & -V_\beta \\ V_\beta & V_\alpha \end{pmatrix} \begin{pmatrix} P_{href} \\ Q_{href} \end{pmatrix} \quad (12)$$

$$i_{ref\,123} = \sqrt{\frac{2}{3}} \begin{pmatrix} 1 & 0 & 1/\sqrt{2} \\ -1/2 & \sqrt{3}/2 & 1/\sqrt{2} \\ -1/2 & -\sqrt{3}/2 & 1/\sqrt{2} \end{pmatrix} i_{h\alpha\beta 0}$$

The power losses occurring inside the cascaded inverter are extracted through a DC-link voltage regulator.

- *The DC-link regulator*

The PV inverter must be able to generate and receive the required energy even while unexpected loads fluctuations. But the injected current relies only on the nature of the load current. Consequently, any current variation results in a considerable rise/drop in dc-link voltages. Thus, the dc voltage balancing plays a fundamental role in inverter efficiency.

An efficient DC-bus regulation needs to achieve two objectives. The first one is maintaining a constant DC voltage value around the reference value. Then, the second goal is overcoming the inverter semi-conductors power losses.

Only one of the dc-link voltages need to be tracked and fed back to get a reliable regulation. The selected controller for the power losses extraction is a PI controller.

- *The current regulator*

The final step to generate the control signal of the PV inverter is the current regulation. The error between the reference currents and the instantaneous injected current by the PV inverter is the input of a PI controller. Then, a PWM gate signals generator, based on the PDPWM modulation technique, produces the switching signals of the cascaded inverter[22].

3. Simulation results and Discussion

In this section, the principal purpose is to check the proposed PV inverter performance. The model of the grid-tied PV system is simulated in Matlab/Simpower systems platform. Several cases have been examined to test the rapidity and the accuracy of the entire system. Three tests are done for checking system flexibility.

3.1. First scenario:

The used network model is the same as [23] that addresses the modelling of PV inverter with a seventeen-level cascaded multilevel structure.

This network choice aims to clarify the proposed structure vulnerabilities and strengths by comparing it with the same architecture used for the same power quality issues. Thus, the control system is committed to making a difference. Two types of load are connected to the grid during the simulation. There are a three-phase diode rectifier TPRD and RL load. The main system parameters for the simulation study are presented in Table 1.

Table 1. Simulation Parameters

The system part	Parameters	Values
Grid	Voltage	6.3 kV
	Frequency	50 Hz
	Supply inductance	1 mH
Loads	TPRD load (R L)	100Ω, 0.6 mH
	Linear load (R L)	100Ω, 600mH
PV panel	SunPower SPR-305	100 Kw, Nsr=5, Npar=66
Active power filter	DC-link parameters (Vdc,Cdc)	(800 V, 1600µF)
	Switching Frequency	20 kHz
	Output Filter (Rf,Lf)	(10Ω, 10 mH)

Similar steps are applied but with a reduced time scale. During the period of 0.55s, the main instances are shown in figure 6.

This simulation presents two modes of operation; the APF and the PV-APF modes. For the first one, the utility supplies only the average components of the active power of the load. Nevertheless, the PV-APF mode requests the injection of both power duties (average and oscillating) by the PV units. Thus, the utility takes charge only of the average energy production. Figure 7 depicts the results of the abovementioned comparison.

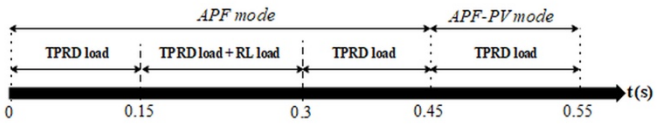

Fig. 6. The simulation modes of operation

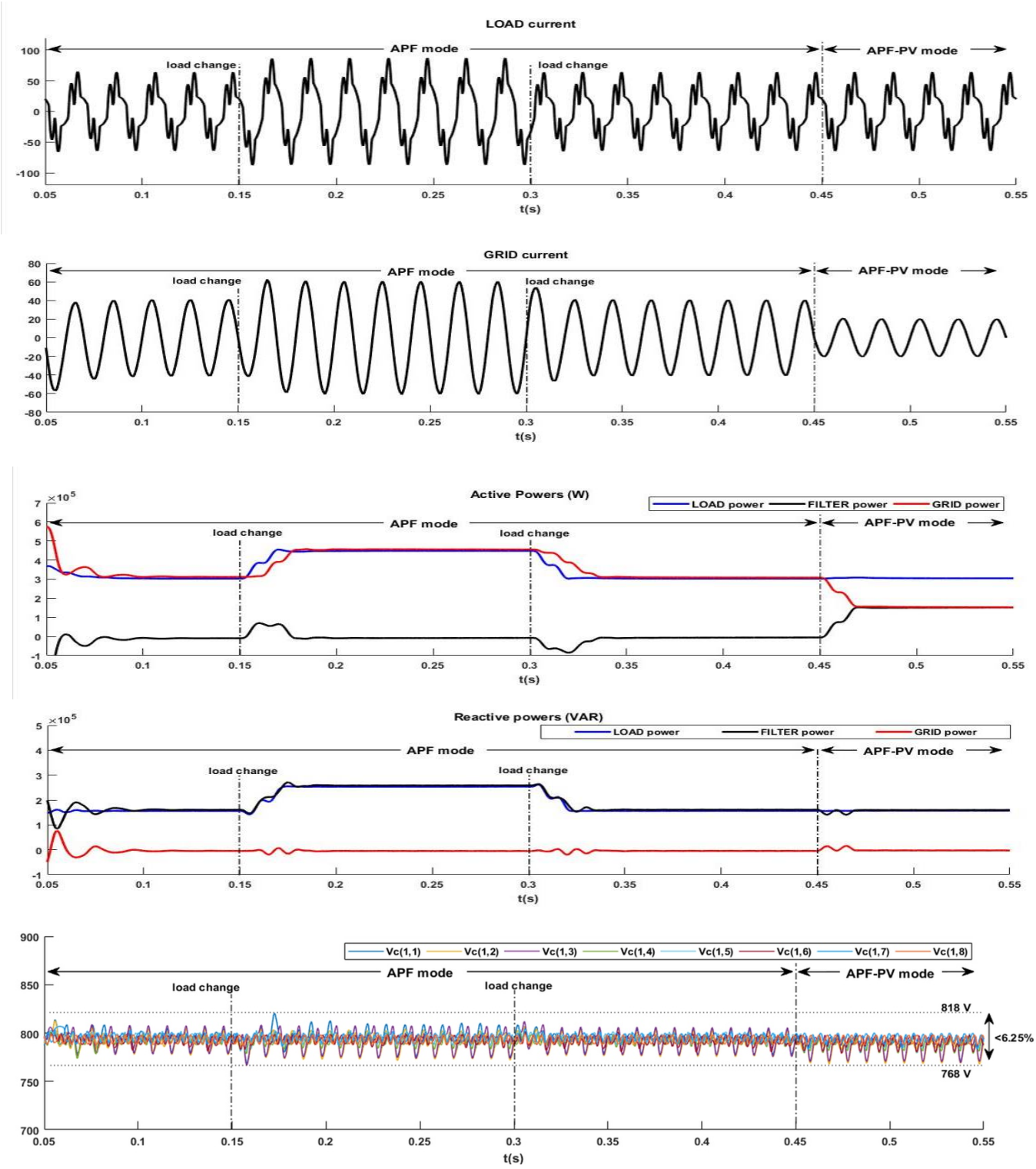

Fig. 7. The simulation results

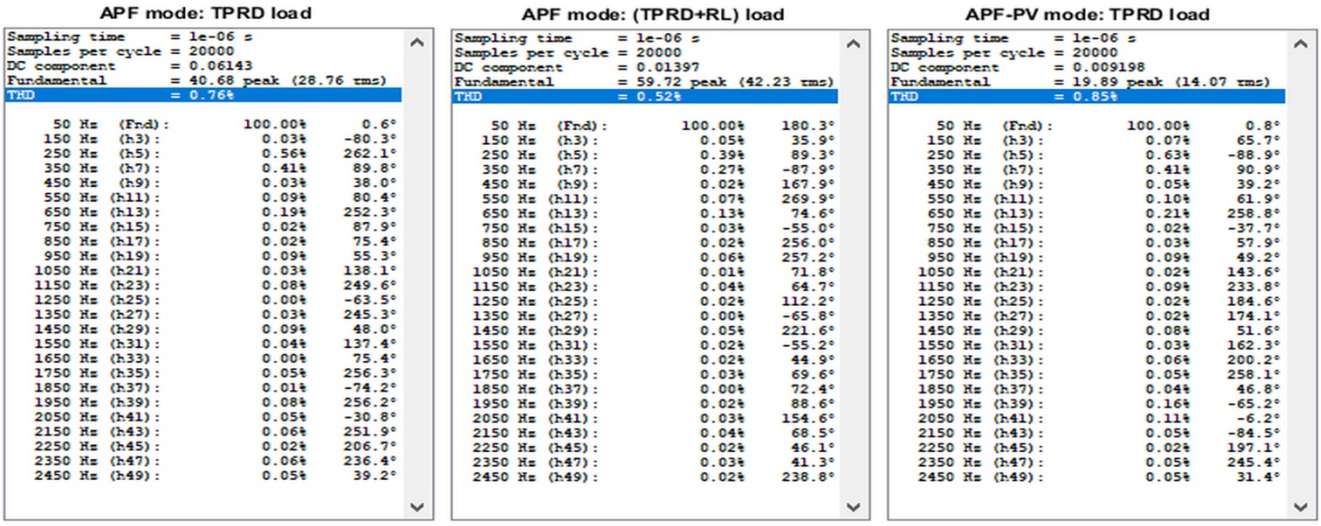

Fig. 8. The THD and the individual harmonic currents values

Table 2. THD values comparison for different cases

Operation modes	Reference model							Proposed model						
	THD (%)	Active power (KW)			Reactive power (KVAR)			THD (%)	Active power (KW)			Reactive power (KVAR)		
		grid	load	filter	grid	load	filter		grid	load	filter	grid	load	filter
APF mode														
TPRD	**1.92**	320	320	-	-	220	220	**0.76**	305	305	-	-	157	157
TPRD + RL load	**1.64**	430	430	-	-	320	320	**0.52**	456	456	-	-	258	258
APF-PV mode														
TPRD	**2.02**	200	320	120	-	220	220	**0.85**	154	305	151	-	157	157

In the stationary phase (t=0.05s), the grid currents keep the sinusoidal waveform regardless of the operating mode. Figure 8 shows the individual harmonic currents (odd harmonics) and the total harmonic distortion values of the grid current for each study case. It appeared that all of them do not exceed the limits set by the IEEE 519-2014 standards[24]. To compare the two models of the PV inverter, Table 2 lists the THD values of the grid currents, and the Reactive and Active powers quantities corresponding to the grid, the load and the PV system. Thus, the simulation results provide an enhancement in the THD values for the different operating modes. The new THD values are less than half of previous ones and not even over 1%. Moreover, the proposed control system shows rapidity in response that is clear in the currents waveform especially at the load state change.

Another aspect to discuss is the voltage balancing. The whole oscillation is inferior to 6.25%. That is achieved by a simplified control thanks to the cascaded multilevel inverter modularity.

Concerning the power delivering by the filter to the grid, the two modes are distinct in the active and reactive power waveforms. For the first mode 'APF mode', the Active power produced by the filter is nearly 0. In the second mode 'APF-PV mode', the required Active power is generated by the PV system besides the grid.

However, the Reactive power is generated by the filter whatever the operating mode. Thus, that leads to enhance also the power factor value which presents important criteria for the power quality.

3.2. Second scenario:

Another scenario is applied to check the inverter performance in different conditions. It is about to validate the inverter flexibility in the case where the number of PV panels is less than the one of inverter cells. Thus, for this test, the model is simulated while changing the number of cascaded multilevel inverter modules to fit with the PV system architecture. Moreover, for each inverter state, different loads are connected to the grid. Besides the used loads in the first test, another TPRD is added to have the simulation steps shown in figure 9.

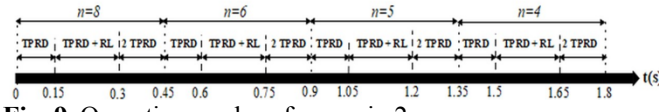

Fig. 9. Operation modes of scenario 2

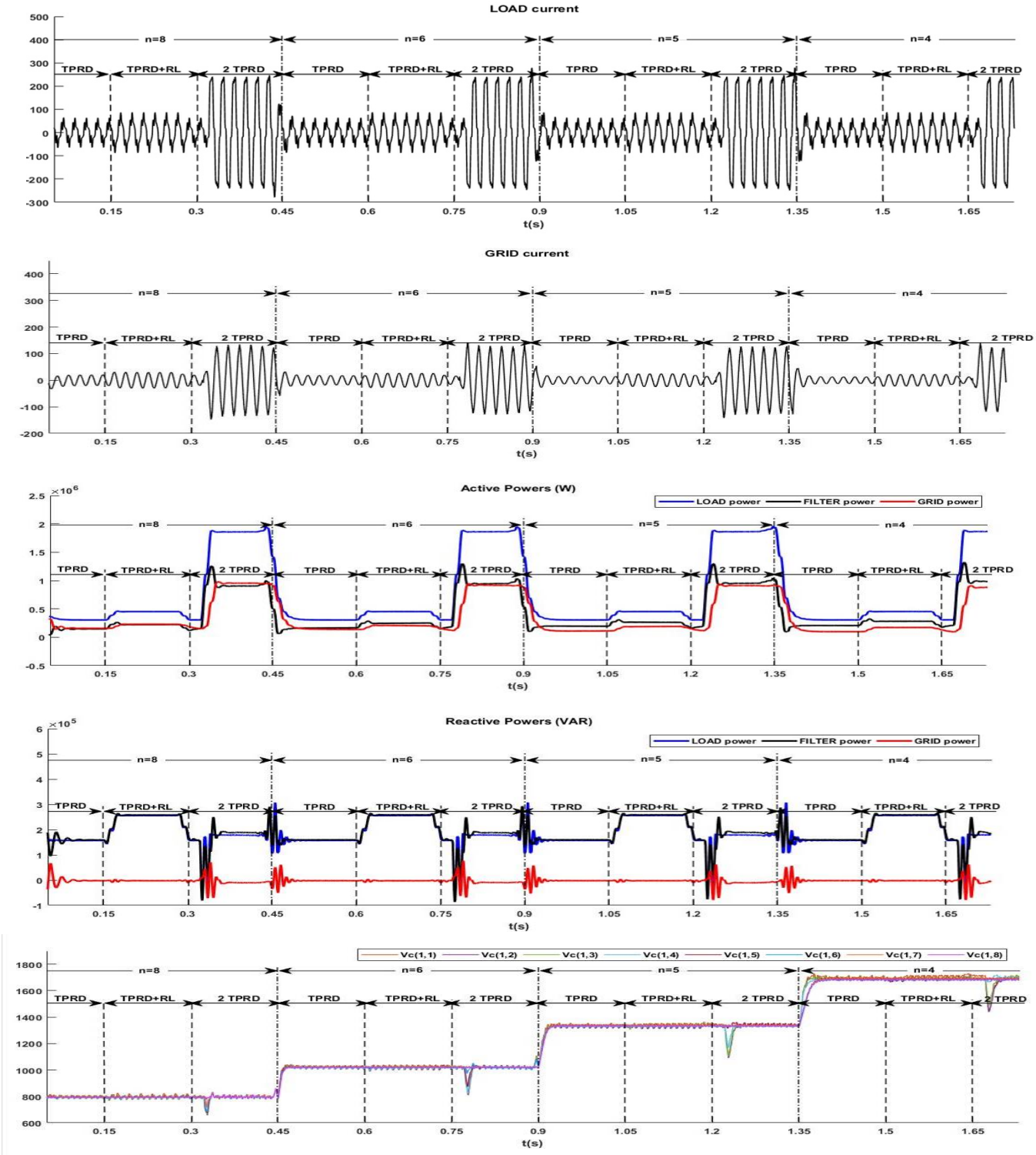

Fig. 10. The simulation results

For this simulation, the PV-APF mode is activated, as shown in Figure 10. The achieved results are satisfying, regardless of the difference in the number of cells. The load currents waveforms are varied, depending on the type of load. However, the grid currents keep a sinusoidal waveform for the different studied cases. Table 3 presents the current THD values of the latter for simulation cases. The values adhere to the limitations established by the IEEE standards. Also, for the different number of cells, they are very close for the two types of load; TPRD load and RL load. However, there is a slight difference in the THD values for the third load, composed of two TPRD.

Moreover, as the first scenario, the control system is characterized by an adequate response time at the load state change and even at the number of cells variation. Also, concerning the delivered active and reactive power, the PV inverter provides its efficiency to feed the electric grid by

approximately the same amount of energy even when decreasing the number of PV arrays.

Table 3. THD values of the grid current for the different simulation state

Operation modes	THD (%)			
	n=8	n=6	n=5	n=4
APF mode				
TPRD	**0.84**	**0.98**	**1.28**	**1.66**
TPRD +RL load	**0.56**	**0.66**	**0.68**	**0.86**
2 TPRD	**1.49**	**2.65**	**1.31**	**3.23**

4. Conclusion

To summarize, the principal function of the Grid-tied PV system is the injection of the active power to the grid to avoid dependence on other energy sources such as fossil fuels. However, by incorporating modifications in the structure and the control system of the PV inverter using for the connection between the grid and the PV system, the functionality of this power stage is increased to cover other roles; active power filter and power factor corrector. Using MATLAB/Simulink, several scenarios are applied to validate the modular PV inverter performance. The starting point is to compare, in similar operation conditions, this inverter with a verified one which has the same structure. This comparison focuses on the observation of the two power devices for different operation modes (PV-APF mode, APF mode) and by applying several loads (TPRD load, RL load). The simulation results show an improvement in terms of rapidity and accuracy for the new model, especially at the load state variation. The cascaded inverter achieves perfectly the two desired functions. The new THD values do not exceed the 1% regardless of the operation modes as well as the connected load. The DC-link voltages are properly balancing. For the second scenario, another option is checked. It is the change in the number of inverter cells to fit the PV system conditions. This simulation is based on the APF-PV mode with the connection of several loads. The results show good performance by keeping a non-disturbed grid even with the variation of the number of the inverter cells. Moreover, the THD values are adequate with the peak value of 3.23%. Also, the results provide the efficient DC voltage regulation as well as the system fast response.

References

[1] S. Kouro, J. I. Leon, D. Vinnikov, and L. G. Franquelo, "Grid-connected photovoltaic systems: An overview of recent research and emerging PV converter technology," *IEEE Industrial Electronics Magazine*, vol. 9, no. 1, pp. 47–61, 2015, doi: doi.org/10.1109/MIE.2014.2376976, . (Article).

[2] C. L. Shen and J. C. Su, "Grid-connection half-bridge PV inverter system for power flow controlling and active power filtering," *International Journal of Photoenergy*, vol. 2012, 2012, doi: 10.1155/2012/760791. (Article).

[3] S. Senguttuvan and M. Vijayakumar, "Solar Photovoltaic System Interfaced Shunt Active Power Filter for Enhancement of Power Quality in Three-Phase Distribution System," *Journal of Circuits, Systems and Computers*, vol. 27, no. 11, 2018, doi: 10.1142/S0218126618501669. (Article).

[4] P. Suresh and G. Vijayakumar, "Shunt Active Power Filter with Solar Photovoltaic System for Long-Term Harmonic Mitigation," *Journal of Circuits, Systems and Computers*, vol. 29, no. 5, Apr. 2020, doi: 10.1142/S0218126620500814. (Article).

[5] R. Noroozian and G. B. Gharehpetian, "An investigation on combined operation of active power filter with photovoltaic arrays," *International Journal of Electrical Power and Energy Systems*, vol. 46, no. 1, pp. 392–399, Mar. 2013, doi: 10.1016/j.ijepes.2012.10.033. (Article).

[6] E. Kabalci, Y. Kabalci, R. Canbaz, and G. Gokkus, "Single phase multilevel string inverter for solar applications," in *2015 International Conference on Renewable Energy Research and Applications, ICRERA 2015*, 2015, pp. 109–114, doi: 10.1109/ICRERA.2015.7418459. (Conference Paper).

[7] M. S. Hamad, K. H. Ahmed, and A. I. Madi, "Current harmonics mitigation using a modular multilevel converter-based shunt active power filter," in *2016 IEEE International Conference on Renewable Energy Research and Applications, ICRERA 2016*, Mar. 2017, pp. 755–759, doi: 10.1109/ICRERA.2016.7884436. (Conference Paper).

[8] V. Fernao Pires, J. Monteiro, and J. Fernando Silva, "A grid-connected PV multilevel cascaded inverter system based on single and three-phase two-level inverters," in *8th International Conference on Renewable Energy Research and Applications, ICRERA 2019*, Nov. 2019, pp.118–123, doi: 10.1109/ICRERA47325.2019.8996765. (Conference Paper).

[9] A. S. Hamed, M. I. Marei, and M. A. Badr, "PV interfacing system based on dual cascaded inverter," in *6th International Renewable Energy Research and Applications, ICRERA 2017*, Dec. 2017, pp. 93–100, doi: 10.1109/icrera.2017.8191211. (Conference Paper).

[10] M. Amin Chitsazan, "Harmonic Mitigation in Three-Phase Power Networks with Photovoltaic Energy Sources," *American Journal of Electrical Power and Energy Systems*, vol. 6, no. 5, p. 72, Aug. 2017, doi: 10.11648/j.epes.20170605.12. (Article).

[11] J. Vaquero, N. Vázquez, I. Soriano, and J. Vázquez, "Grid-connected photovoltaic system with active power filtering functionality," *International Journal of Photoenergy*,vol.2018,2018, doi: 10.1155/2018/2140797. (Article).

[12] M. Hlaili and H. Mechergui, "Comparison of Different MPPT Algorithms with a Proposed One Using a Power Estimator for Grid Connected PV Systems," *International Journal of Photoenergy*, vol. 2016, 2016, doi: 10.1155/2016/1728398. (Article).

[13] S. Salman, X. Ai, and Z. Wu, "Design of a P-&-O algorithm based MPPT charge controller for a stand-

alone 200W PV system," *Protection and Control of Modern Power Systems*, vol. 3, no. 1, p. 25, Dec. 2018, doi: 10.1186/s41601-018-0099-8. (Article).

[14] A. Gaga, F. Errahimi, and N. Es-Sbai, "Design and implementation of MPPT solar system based on the enhanced P&O algorithm using Labview," in *Proceedings of 2014 International Renewable and Sustainable Energy Conference, IRSEC 2014*, Mar. 2014, pp. 203–208, doi: 10.1109/IRSEC.2014.7059786. (Conference Paper).

[15] P. Kinjal, K. B. Shah, and G. R. Patel, "Comparative analysis of P&O and INC MPPT algorithm for PV system," Sep. 2015, doi: 10.1109/EESCO.2015.7253982. (Conference Paper).

[16] D. Beriber and A. Talha, "MPPT techniques for PV systems," in *International Conference on Power Engineering, Energy and Electrical Drives*, 2013, pp. 1437–1442, doi: 10.1109/PowerEng.2013.6635826. (Conference Paper).

[17] L. F. N. Lourenco, M. B. de Camargo Salles, R. M. Monaro, and L. Queval, "Technical cost of PV-STATCOM applications," in *6th International Conference on Renewable Energy Research and Applications, ICRERA 2019*, Dec. 2017, pp. 534–538, doi: 10.1109/icrera.2017.8191118. (Conference Paper).

[18] S. Rajani and K. Swarnalatha, "A New Topology For Capacitor Voltage Regulation In Cascaded H-Bridge Multilevel Converters With Fuzzy Logic Controller," *INTERNATIONAL JOURNAL OF PROFESSIONAL ENGINEERING STUDIES*, vol. V, no. 4, 2015. (Article).

[19] M. A. A. M. Zainuri *et al.*, "Photovoltaic integrated shunt active power filter with simpler ADALINE algorithm for current harmonic extraction," *Energies*, vol. 11, no. 5, 2018, doi: 10.3390/en11051152. (Article).

[20] F. A. D. M. Soomro, S. C. Chong, Z. A. Memon, M. A. Uqaili, "Performance of Shunt Active Power Filter Based on Instantaneous Reactive Power Control Theory for Single-Phase System," *International Journal of Renewable Energy Research (IJRER)*, vol. 7, no. 4, pp. 1741–1751, 2017. (Article).

[21] G. F. NGUYEN DUC TUYEN, "PV-Active Power Filter Combination Supplies Power to Nonlinear Load and Compensates Utility Current NGUYEN," *IEEE Power and Energy Technology Systems Journal*, vol. 2, pp. 1–11, 2015, doi: 10.1109/JPETS.2015.2404355. (Article).

[22] L. Chaturvedi, D. K. Yadav, and G. Pancholi, "Comparison of SPWM,THIPWM and PDPWM technique based voltage source inverters for application in renewable energy," *Journal of Green Engineering*, vol. 7, no. 1–2, pp. 83–98, 2017, doi: 10.13052/jge1904-4720.7125. (Article).

[23] T. Demirdelen, R. İ. Kayaalp, and M. Tumay, "Simulation modelling and analysis of modular cascaded multilevel converter based shunt hybrid active power filter for large scale photovoltaic system interconnection," *Simulation Modelling Practice and Theory*, vol. 71, pp. 27–44, Feb. 2017, doi: 10.1016/j.simpat.2016.11.003. (Article).

[24] IEEE Standard 519-2014, Recommended Practice and Requirements for Harmonic Control in Electric Power Systems, *The Institute of Electrical and Electronics Engineers*, 2014.(Standards and Reports).